PHILOSOPHICAL TRANSACTIONS OF THE ROYAL SOCIETY A MATHEMATICAL, PHYSICAL & ENGINEERING SCIENCES

Dynamics of dislocations in a two-dimensional block copolymer system with hexagonal symmetry

Aldo D. Pezzutti, Daniel A. Vega and Marcelo A. Villar

Phil. Trans. R. Soc. A 2011 **369**, 335-350
doi: 10.1098/rsta.2010.0269

PHILOSOPHICAL TRANSACTIONS OF THE ROYAL SOCIETY A

Phil. Trans. R. Soc. A (2011) **369**, 335–350
doi:10.1098/rsta.2010.0269

Dynamics of dislocations in a two-dimensional block copolymer system with hexagonal symmetry

By Aldo D. Pezzutti[1], Daniel A. Vega[1,*] and Marcelo A. Villar[2]

[1]*Instituto de Física del Sur, Department of Physics, and* [2]*Planta Piloto de Ingeniería Química (PLAPIQUI), Department of Chemical Engineering, Universidad Nacional del Sur – CONICET, Avenida L.N. Alem 1253, (8000) Bahía Blanca, Argentina*

Block copolymer thin films have attracted considerable attention for their ability to self-assemble into nanometre-scale architectures. Recent advances in the use of block copolymer thin films as nano-lithographic masks have driven research efforts in order to have better control of long-range ordering in the plane of the film. Irrespective of the method of sample preparation, different quasi-two-dimensional systems with hexagonal symmetry unavoidably contain translational defects, called dislocations. Dislocations control the process of coarsening in the nano/meso-scales and provide one of the most important mechanisms of length-scale selection in hexagonal patterns. Although in the last decade the nonlinear dynamics of topological defects in quasi-two-dimensional systems has witnessed significant progress, still little is known about the role of external fields on the creation and annihilation mechanisms involved in the relaxation process towards equilibrium states. In this paper, the dynamics of dislocations in non-optimal hexagonal patterns is studied in the framework of the Ohta–Kawasaki model for a diblock copolymer. Measurements of the climb and glide velocities as a function of the wave vector deformation reveal the main mechanisms of relaxation associated with the motion of dislocations.

Keywords: dynamics of defects; dislocations; diblock copolymer; hexagonal symmetry; penta–hepta defects

1. Introduction

Diblock copolymers consist of two homogeneous but chemically distinct macromolecular blocks connected by a covalent bond. During the last decades, it has been clearly established that even slightly dissimilar blocks can lead to phase separation at the nano-scale. In this case, it has been found that the volume fraction of each block largely sets the microdomain morphology [1–4]. For example, body-centred cubic arrays of spheres (of $Im\bar{3}m$ symmetry), hexagonally packed cylinders, lamellar and gyroid phases (cubic symmetry $Ia\bar{3}d$)

*Author for correspondence (dvega@uns.edu.ar).

One contribution of 17 to a Theme Issue 'Nonlinear dynamics in meso and nano scales: fundamental aspects and applications'.

have been observed [5]. Theoretical modelling with a self-consistent field theory has successfully described the existence of these equilibrium structures [4]. It has been found that the phase diagram for a diblock copolymer with equal segment lengths is a function only of the volume fraction of one of the components and χN, where N is the total number of statistical segments and χ is the dimensionless Flory interaction parameter describing the enthalpic interactions.

During the last decade, block copolymer thin films have attracted considerable attention for their ability to self-assemble into highly regular structures [6–11]. For example, block copolymer thin films are of interest as large-area nanolithographic masks, which are inaccessible via standard lithographic techniques [11,12]. However, one of the main drawbacks of the method is related to lack of long-range order [13,14]. Since block copolymer domains nucleate at random positions with a random orientational phase, the appearance of topological defects at the interfaces of different domains is completely unavoidable, and several strategies, such as graphoepitaxy or external ordering fields, have been employed to obtain ordered hexagonal and lamellar masks with a low density of topological defects [11,12]. For example, by employing a shearing technique, Angelescu *et al.* [13] showed that thin films of sphere-forming block copolymers can be well aligned over square-centimetre regions. Compared with thermal treatments, where the density of topological defects can hardly be reduced below 200 dislocations per square micrometre, in shear-aligned hexagonal patterns the orientational order was perfect over a $2.5 \times 2.5\,\mu m^2$ area while the translational order was limited only by the presence of a reduced number of dislocations (on average six dislocations per square micrometre).

Block copolymer thin films have also proved to be very important from a fundamental point of view to unveil the mechanisms leading to phase equilibrium [15] and ordered structure [8,16,17] in quasi-two-dimensional systems. The macromolecular nature of polymers reduces effects related to the atomic details, and, compared with other self-assembling systems, such as lyotropic liquid crystals, block copolymer melts are blessed with a number of advantages and their behaviour is more universal.

Although there has been recent progress in understanding equilibrium phenomena and the mechanisms by which order evolves in a two-dimensional smectic system after being quenched from the disordered state, still little is known about the kinetic pathways leading to equilibrium in hexagonal phases [17,18]. Previously, it was found that in planar systems with smectic symmetry the orientational correlation length of the domains grows with the average spacing between disclinations according to a power law [6,7]. In this case, the orientational correlation length is controlled by the density of disclinations and the dominant mechanism of ordering involves the annihilation of tripoles and quadrupoles of disclinations [7]. Since the process of disclination annihilation is mediated by the diffusion of dislocations, the densities of disclinations and dislocations and the orientational order parameter show a power-law dependence on time.

On the other hand, in hexagonal patterns the dynamics is more subtle because most of the defects are condensed along grain boundaries and the strain field of the defects becomes short-ranged [7,16].

In 1962, Lifshitz predicted the possibility of formation of a stable lattice of domains as a consequence of dynamical frustration in reaching equilibrium [19]. According to this model, as a consequence of the relaxation driven by

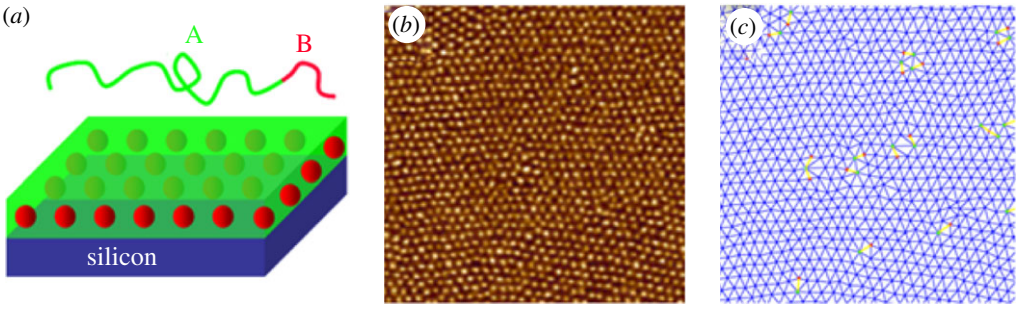

Figure 1. (*a*) Schematic of an A–B diblock copolymer and a single-layer block copolymer thin film with spherical morphology. Each molecule consists of a block of polymer A (green) joined covalently to a smaller block of polymer B (red). The copolymer self-assembles into a hexagonal structure of spherical domains of polymer B surrounded by a continuous domain of polymer A. (*b*) Typical AFM phase contrast image of an approximately 30 nm thick poly(styrene)-*b*-poly(isoprene) block copolymer thin film. The poly(styrene) spheres organize themselves into a single layer, hexagonally packed with an average spacing between spheres of approximately 30 nm [23]. (*c*) Through a Delaunay triangulation of the domain structure in (*b*), it is possible to determine the number of dislocations in the system. For the hexagonal phase, dislocations are defined as pairs of spheres with five and seven nearest neighbours separated by a lattice constant. Spheres with seven neighbours are indicated with a green dot, those with five neighbours in red and dislocations by a connecting pale yellow line segment. (Online version in colour.)

the curvature of grain boundaries, triple points (bounded regions where three grains with different orientations meet) can become pinned to their positions, slowing down the dynamics. The analysis of the dynamics of a system with p degenerate states depicting Lifshitz's configurations was theoretically studied by Safran [20]. According to this model, the domains grow with a power law in time for $p < d + 1$ (d being the spatial dimension), but logarithmically in time in the case $p \geq d + 1$ [17,21,22].

In two-dimensional systems with hexagonal symmetry, the Lifshitz–Safran model predicts that the dynamics is controlled by the triple points [17]. The role of the triple points on the coarsening process at long times have been studied numerically and experimentally. Numerical simulations with a Cahn–Hilliard model showed the same features as those proposed by Lifshitz, with orientational and translational correlation lengths growing logarithmically in time [17,21]. Similar features were found by Harrison *et al.* [8] in block copolymer thin films of a sphere-forming block copolymer (figure 1). In this study, the annealing process after a quench from the disordered state was analysed by electron microscopy and time-lapse atomic force microscopy (AFM) on a system that is schematically shown in figure 1*a* [8]. By taking advantage of the modulus difference between the two blocks, it is possible to use AFM in the tapping mode to image the microdomain pattern (figure 1*b*) and to track the coarsening mechanism. Both experiments and simulations with a Cahn–Hilliard model showed that disclinations condense into dislocations and most dislocations condense into grain boundaries [8,16]. The dynamics involves the interplay of disclinations and lines of dislocations, and the most frequently observed process of coarsening is the collapse of a smaller grain that resides on the boundary of two larger grains. Then, irrespective of the mechanism behind the process of coarsening, the dynamics always involves the diffusion of dislocations.

In this work, the motion of dislocations in slightly deformed hexagonal patterns is analysed. The study is carried out by means of a Cahn–Hilliard model [24] for a diblock copolymer (Ohta–Kawasaki free-energy functional [25]).

2. Dynamical model

Let us consider a block copolymer consisting of two homopolymer blocks A and B (degree of polymerization N_A and N_B, respectively) quenched from the high-temperature disordered melt into the unstable region of the phase diagram. The total degree of polymerization is $N = N_A + N_B$.

One of the simplest models proposed to describe the dynamics of micro-phase separation for this system is to consider the Ohta–Kawasaki free-energy functional together with a Langevin dynamics for a conserved order parameter [25–28]:

$$\frac{\partial \psi}{\partial t} = M\nabla^2\left(\frac{\delta F}{\delta \psi}\right) + \zeta(\mathbf{r}, t). \tag{2.1}$$

Here, the order parameter ψ is defined in terms of the local densities of each block in the block copolymer,

$$\psi(\mathbf{r}, t) = \frac{\rho_A(\mathbf{r}, t) - \rho_B(\mathbf{r}, t)}{2\rho_0}, \tag{2.2}$$

where $\rho_A(\mathbf{r}, t)$ and $\rho_B(\mathbf{r}, t)$ are the local segment densities of the blocks A and B, respectively, M is a phenomenological mobility coefficient, and ζ is a random noise term, with zero average and second moment related to the mobility coefficient and the noise strength η_0 through the fluctuation–dissipation relationship [29]:

$$\langle \zeta(\mathbf{r}, t)\zeta(\mathbf{r}', t')\rangle = 2M\eta_0\delta(\mathbf{r} - \mathbf{r}')\delta(t - t'). \tag{2.3}$$

The free-energy functional $F(\psi)$ splits as

$$F(\psi) = F_s(\psi) + F_\ell(\psi), \tag{2.4}$$

where terms model short- and long-range interactions. The long-range free-energy contribution arises from the chain connectivity of two blocks and can be expressed as [25]

$$F_\ell(\psi) = \frac{\beta}{2}\int \mathrm{d}\mathbf{r}'\,\mathrm{d}\mathbf{r}\, G(\mathbf{r} - \mathbf{r}')\psi(\mathbf{r})\psi(\mathbf{r}'), \tag{2.5}$$

where $G(\mathbf{r})$ is a solution of $\nabla^2 G(\mathbf{r}) = -\delta(\mathbf{r})$. The short-range term has the typical Landau form,

$$F_s(\psi) = \int \mathrm{d}\mathbf{r}\left[H(\psi) + \frac{D}{2}|\nabla\psi|^2\right], \tag{2.6}$$

where $H(\psi)$ stands for the mixing free energy of the homogeneous blend of disconnected A–B homopolymers, and $(D/2)|\nabla\psi|^2$ represents the free-energy cost

for spatial composition inhomogeneity. The positive constant D scales with the Kuhn statistical segment length b as $D \propto b^2$ [25,28]. Here $H(\psi)$ takes the form:

$$H(\psi) = \tfrac{1}{2}[-\tau + A(1-2f)^2]\psi^2 + \tfrac{1}{3}\lambda(1-2f)\psi^3 + \tfrac{1}{4}\sigma\psi^4. \tag{2.7}$$

The parameters A, λ, β and σ are related to the vertex functions derived by Leibler [30]. The constant f is the block copolymer asymmetry [25] and the parameter τ depends linearly on the Flory–Huggins parameter χ and provides a measurement of the depth of quench. In this free-energy model, which belongs to the Brazovskii class [31], the disordered phase becomes unstable to periodic modulations just as the block copolymer melt traverses the spinodal line. By mapping the Leibler free-energy functional [30] onto the Brazovskii free-energy expression, Fredrickson & Helfand [32] and Podneks & Hamley [33] were able to extract fluctuation corrections for block copolymers. It was found that the Brazovskii fluctuations modify the phase behaviour in the neighbourhood of the critical point and that the order–disorder transition temperature moves the critical line towards higher temperatures.

In this work, equation (2.1) was numerically solved by the cell dynamics method on a two-dimensional square lattice [34–37]. According to this approach, the evolution of the order parameter ψ can be expressed as

$$\psi(\mathbf{n}, t+1) = \Gamma(\psi(\mathbf{n}, t)) - \langle\langle \Gamma(\psi(\mathbf{n}, t)) - \psi(\mathbf{n}, t)\rangle\rangle - \beta\psi(\mathbf{n}, t), \tag{2.8}$$

where

$$\Gamma(\psi(\mathbf{n}, t)) = f(\psi(\mathbf{n}, t)) + D[\langle\langle\psi(\mathbf{n}, t)\rangle\rangle - \psi(\mathbf{n}, t)] \tag{2.9}$$

and $f(\psi(\mathbf{n}, t))$ is given by

$$f(\psi) = [1 + \tau - A(1-f)^2]\psi - \lambda(1-2f)\psi^3 - \sigma\psi^4. \tag{2.10}$$

Here, $\mathbf{n} = (n_x, n_y)$ designates the lattice points and $\langle\langle\Xi\rangle\rangle$ represents an average over all neighbours of an arbitrary function Ξ, and is related to the isotropic Laplacian through

$$\nabla^2\Xi = 3[\langle\langle\Xi\rangle\rangle - \Xi]. \tag{2.11}$$

For a two-dimensional system,

$$\langle\langle\Xi\rangle\rangle = \frac{1}{6}\sum_{\mathrm{s}\in\mathrm{NN}}\Xi(\mathbf{s}) + \frac{1}{12}\sum_{\mathrm{s}\in\mathrm{NNN}}\Xi(\mathbf{s}), \tag{2.12}$$

where NN and NNN represent the nearest-neighbour and next-nearest-neighbour lattice sites, respectively.

In this work, the block copolymer composition was fixed at $f = 0.45$, and the phenomenological parameters were fixed at $A = 1.5$, $\sigma = 0.38$, $\lambda = 0.23$, $D = 0.3$ and $\beta = 0.03$. The noise term was ignored. We have also conducted studies that include thermal fluctuations and have confirmed that fluctuations renormalize the depth of quench [38]. The two-dimensional mean-field equilibrium structure for these parameters is a hexagonal array of domains characterized by a dominant wavenumber k_0 ($k_0^4 = \beta/D$). We used a 512×512 lattice system with periodic boundary conditions.

3. Linear instability analysis

To analyse the stability of the hexagonal patterns and to gain insight into the different transition mechanisms, in this section we perform a simplified single-wavenumber, amplitude equation analysis, which considers only the essential symmetries of the problem.

Periodic hexagonal patterns are expected to have a finite region of stability. As shown below, if the temperature of quench and wavenumber disturbances are small, the hexagonal pattern is stable. On the other hand, if the temperature of quench or wavenumber disturbances are moderately increased, different types of instabilities may appear in the system to relax the free-energy excess. One such instability is the so-called Eckhaus instability, where the optimal wavenumber of the system may be recovered through the nucleation and diffusion of topological defects.

In block copolymer melts, the stability and dynamics towards equilibrium of different phases have been numerically studied by Qi & Wang [39]. In that study, it was found that geometric characteristics of the free-energy surface are responsible for the non-trivial intermediate states on the kinetic pathways. For example, it was found that transitions from the lamellar phase to the hexagonal phase may go through an intermediate metastable phase (perforated lamella).

For a generic system governed by a Ginzburg–Landau free energy, the different instabilities of two-dimensional hexagonal patterns have been extensively studied by Sushchik & Tsimring [40].

A perfect hexagonal system can be represented as the superposition of three plane waves oriented at 120° with respect to each other. Thus, the order parameter ψ for a slightly disturbed hexagonal pattern can be written in the form

$$\psi(\mathbf{r},t)=\sum_{j=1}^{3}A_j(\mathbf{r},t)\exp[\mathrm{i}(\mathbf{k}_j+\mathbf{K}_j)\mathbf{r}]+\text{c.c.}, \tag{3.1}$$

where $A_j(\mathbf{r},t)$ are slowly varying envelopes and $|k_j|=k_0$, with $\mathbf{k}_1=k_0\hat{x}$ and the other vectors $\mathbf{k}_2$ and $\mathbf{k}_3$ are obtained from this by rotations of $\pm 2\pi/3$ (resonant condition). Here, we choose $K_j=\mathbf{K}_j.\mathbf{e}_j$ to be the wavenumber disturbance from the optimum wavenumber values $\mathbf{k}_j$ ($\mathbf{e}_j$ is the unit vector oriented along the wavevector of mode j: $\mathbf{e}_j=\mathbf{k}_j/k_j$). Particularly, here we only analyse the case where $\mathbf{K}_1+\mathbf{K}_2+\mathbf{K}_3=0$.

Substituting equation (3.1) into equation (2.4) and expanding the long-range free-energy contribution, the free energy of the system can be expressed in the Sushchik & Tsimring form in terms of the amplitudes $A_j(\mathbf{r},t)$ as

$$\begin{aligned}F=\int \mathrm{d}\mathbf{r}\,[&-\mu(|A_1|^2+|A_2|^2+|A_3|^2)-(A_1^*A_2^*A_3^*+\text{c.c.})\\&+\tfrac{1}{2}(|A_1|^4+|A_2|^4+|A_3|^4)+\gamma(|A_1|^2|A_2|^2+|A_1|^2|A_3|^2\\&+|A_2|^2|A_3|^2)+(|D_1A_1|^2+|D_2A_2|^2+|D_3A_3|^2)],\end{aligned} \tag{3.2}$$

where $D_j=\mathrm{i}K+\partial_{Xj}$ (see [40] for more details about the approximations involved in equation (3.2)).

The temporal evolution of the amplitude equations can be variationally expressed as

$$\frac{\partial A_i}{\partial t} = -\frac{\delta F}{\delta A_i}. \tag{3.3}$$

Following the Sushchik & Tsimring approach [40], it can be shown that the ordered structures become unstable above the line given by

$$K^2 = \frac{2[\tau - A(1-2f)^2 - 2\sqrt{\sigma D}]6\sigma}{[4\lambda(1-2f)]^2} + \frac{1}{4(1+2\gamma)}. \tag{3.4}$$

On the other hand, the region where the hexagonal phase is stable is delimited by the line

$$K^2 = \frac{1}{4(1+2\gamma)}\left[1 + 4\mu + 8\mu\gamma - \frac{[-\gamma - 2 + (1+2\gamma)\sqrt{24\mu(1+\gamma)+1}]^2}{9(1+\gamma)^2}\right], \tag{3.5}$$

where $\mu = 3[\tau - A(1-2f)^2 - 2\sqrt{\beta D}]\mu/[4\lambda^2(1-2f)^2]$.

In addition, it has been found that the Eckhaus instability can also trigger a transition from the hexagonal phase to the stripped phase (smectic symmetry) as the depth of quench τ overcomes the hexagonal/smectic line:

$$\tau^* = \frac{3}{8}\frac{3\gamma + 1 + \sqrt{2}(\gamma+1)^{3/2}}{(1+2\gamma)(\gamma-1)^2}[\lambda(1-2f)]^2\sigma + A(1-2f)^2 + 2\sqrt{\beta D}. \tag{3.6}$$

Figure 2 shows the stability diagram for the hexagonal phase as a function of the depth of quench τ. In this diagram, we can distinguish four different regions corresponding to different instabilities. Although other instabilities can also be identified [40], this study is mainly focused on the region where the hexagonal phase is stable.

To study the kinetics of the morphological transitions numerically, we start the simulations with a perfect hexagonal crystal with a non-optimal wavenumber. Real-space images show that, when the difference between the wavenumber K and k_0 is small, the system remains in the stable zone, and the pattern shows no indication of any distortion. However, when the difference between the wavenumber and k_0 is large, the crystal becomes unstable and, depending on temperature, different relaxational mechanisms can be triggered.

We have analysed the stability of the hexagonal phase through the circularly averaged scattering function $S(k)$. Here $S(k)$ was determined as $S(k) = \langle\tilde{\psi}(\mathbf{k})\tilde{\psi}(\mathbf{k})^*\rangle$, where $\tilde{\psi}(\mathbf{k})$ represents the Fourier transform of the order parameter. The main results are shown in figure 3.

At shallow quenches ($\tau \sim \tau_c$) and $K \sim 0$ the hexagonal pattern is stable. Figure 3 shows the scattering function $S(k)$ for a hexagonal pattern located in this region (region I of figure 2). As expected, the scattering function is sharply peaked at k_0. It is also possible to observe higher-order peaks at the positions expected for the hexagonal crystalline structure (k_0, $\sqrt{3}k_0$, $\sqrt{7}k_0$) [16].

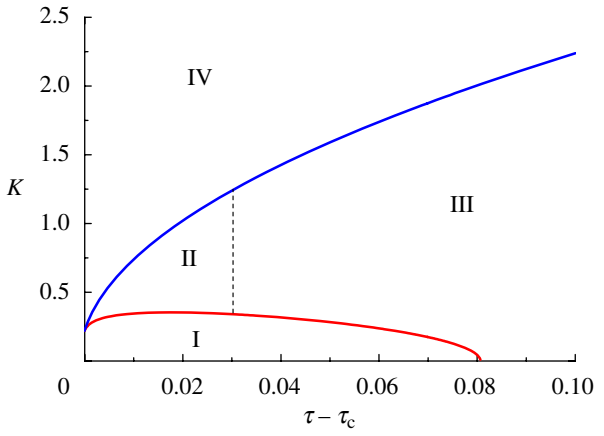

Figure 2. Stability region of hexagonal patterns as a function of the depth of quench τ. The lower line (zone I) is the existence line of hexagons. At shallow quenches and small wavevector distortions, the pattern is reconstructed through the spontaneous creation of pairs of dislocations (zone II). At deeper quenches, the hexagonal pattern is reconstructed into a lamellar (smectic) phase (zone III). In zone IV, the hexagonal pattern is completely unstable. Here τ_c indicates the position of the spinodal line. (Online version in colour.)

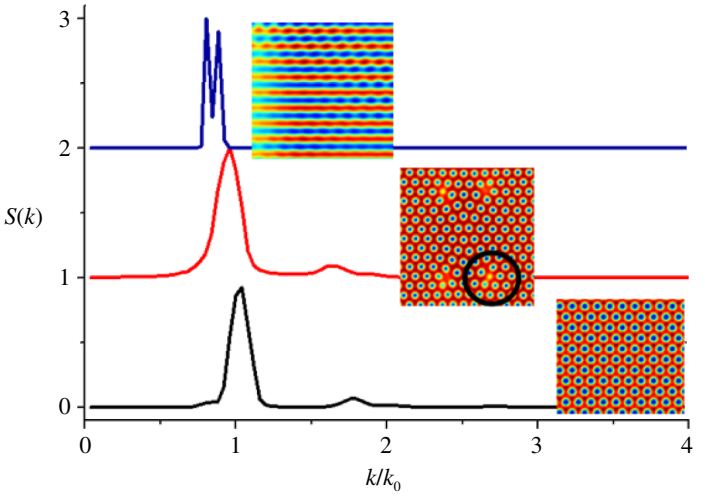

Figure 3. Circularly averaged scattering function $S(k/k_0)$ (arbitrary intensity scale). Here, wavevector k_0 is the optimal wavenumber value in the stable region I ($\tau - \tau_c = 10^{-4}$, $K = 0$). Bottom: hexagonal system at equilibrium ($\tau - \tau_c = 10^{-4}$, $K = 0$). Centre: when τ and K locate the system in region II of figure 2 ($\tau - \tau_c = 10^{-2}$, $K = 0.5$), the pattern recovers its optimal wavevector via the creation of pairs of dislocations with opposite Burgers vectors. The circle in the pattern emphasizes the presence of one of the four dislocations created through this mechanism. Top: in region III, the hexagonal pattern becomes unstable and the domains melt into a lamellar structure ($\tau - \tau_c = 4 \times 10^{-2}$, $K = 0.5$). (Online version in colour.)

At a given temperature, if the wavenumber disturbance K is relatively small, we observed that the pattern becomes unstable and there is a spontaneous creation of pairs of dislocations (region II, $K = 0.5$ and $\tau - \tau_c = 10^{-2}$). In this case, we can observe that the main peak of the scattering function moves towards the low-k region while the hexagonal symmetry remains stable, as evidenced by the presence of the high-order peaks in $S(k)$. Then, the pattern is reorganized into a new hexagonal pattern via the annihilation of crystalline planes mediated by the creation and diffusion of dislocations. At deeper quenches (region III, $K = 0.5$ and $\tau - \tau_c = 4 \times 10^{-2}$), the hexagonal pattern suffers a hexagonal to stripes transition. In figure 3, we can observe that the main peak of the scattering function splits into two, one corresponding to the primitive hexagonal pattern and the other corresponding to a lamellar phase. Then, in this region the hexagonal phase goes into the lamellar equilibrium phase with a wavenumber smaller than k_0. Finally, if the wavenumber disturbance K increases beyond the limits of stability of the ordered phase (region IV), we have observed that ordered structures become unstable.

4. Dislocation dynamics under stress

The microstructure of a condensed phase and the distribution of topological defects largely determine its mechanical, transport and thermodynamic response, as well as the temporal evolution of its non-equilibrium configurations.

In the case of lamellar patterns, the dislocations play an important role in the pattern selection process. For an isolated dislocation in a system with lamellar structure, the pattern can be divided into two regions A and B, with different wavenumbers k_a and k_b, respectively. Let us suppose that region B contains an extra lamella. If the defect does not move, the pattern has an optimal wavenumber located between q_a and q_b. On the other hand, if q_a or q_b are the preferred wavenumbers of the system, the dislocation climbs in order to add or remove the extra lamella. In the presence of external fields, the dislocation can also glide normally to the lamellae. In this case, the overall wavenumber of the pattern does not necessarily change during the diffusional motion of the dislocation.

The elementary defects of a two-dimensional hexagonal system are disclinations (orientational defects). These are point defects formed by a domain having a number of nearest neighbours different from six, typically five (negative disclination) or seven (positive disclination). In addition to disclinations, dislocations (translational defects) are also present. Dislocations are composed defects formed by a pair of disclinations of opposite sign separated by a lattice constant.

Owing to the underlying crystalline lattice, the energy of the dislocation oscillates as a function of its position so that it can move only if the forces overcome the periodic Peierls potential [41]. The motion of dislocations can be separated into two different mechanisms: climb and glide. In the climb process, the velocity of the dislocation is parallel to the axis of the dislocation (perpendicular to the Burgers vector) and requires the diffusion of point defects. Glide is the motion perpendicular to the axis of the dislocation (parallel to the dislocation's Burgers vector). Since glide requires only a local rearrangement of the system, the diffusion constants for glide are expected to be much larger than those for climb.

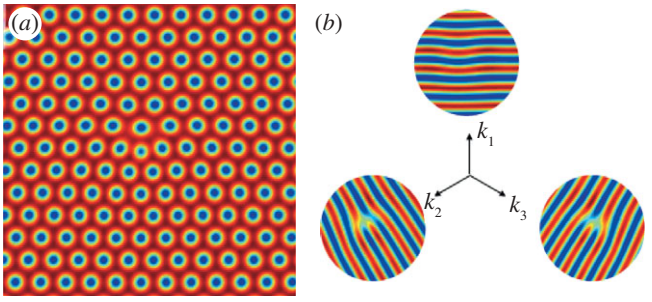

Figure 4. Decomposition of a hexagonal pattern with a dislocation into three plane waves oriented at 120° with respect to one another. The hexagonal pattern with a dislocation embedded near its centre shown in (*a*) can be obtained as the superposition of the three patterns shown in (*b*). The k_2 and k_3 lamellae have dislocations, while the k_1 lamellae are dislocation-free. The two dislocations have opposite winding numbers. (Online version in colour.)

When the wavenumber of the hexagonal system is optimal, the dislocations remain immobile. When the wavenumber is not optimal, the defects move in order to adjust the wavenumber of the pattern back into the stability region. The defect motion can be driven by the superposition of two Peach–Köhler forces, corresponding to the two singular modes.

Here, we studied the dynamics of dislocations under different conditions of deformation. We apply external stress on a hexagonal structure containing a dislocation by deforming it in a particular direction.

Since the hexagonal pattern can be written in the form $\psi = \sum_{j=1}^{3} A_j \exp(\mathrm{i}k_j r) +$ c.c., the dislocation in the hexagonal system can be thought of as the bound state of two 'lamellar dislocations' of opposite winding numbers. Here, the $\mathbf{k}_i$ are the wavevectors corresponding to the three lamellar patterns. These vectors are oriented at 120° with respect to each other and satisfy the resonance condition $\mathbf{k}_1 + \mathbf{k}_2 + \mathbf{k}_3 = 0$ (see scheme of figure 4).

To analyse the dynamics, we considered the dislocation as formed by a negative dislocation in mode 2 and a positive dislocation in mode 3. Mode 1 contains no dislocations. Then, the motion of the dislocation is studied by considering a shallow quench into the spinodal region (the depth of quench is fixed at $\tau - \tau_c = 10^{-4}$). Given the proximity to the spinodal, the system shows a very strong wavenumber selectivity at $k = k_0$. We found that dislocations remain immobile when the amplitudes of the three wavenumbers k_i equal the dominant wavenumber of the symmetry-breaking instability k_0 (i.e. $k_i = |k_0|$).

Here, the motions of the defects were tracked by filtering individual pairs of Bragg peaks in the Fourier transform and then performing an inverse Fourier transform to identify the dislocations present in each set of lamellae (characterized by wavevectors $\mathbf{k}_1$, $\mathbf{k}_2$ and $\mathbf{k}_3$).

Similarly to lamellar patterns, in hexagonal systems the motion of the dislocations depends on the wavenumber distortions to k_0. Here, we considered three distinct initial conditions with a non-optimal wavenumber configuration. As shown below, both the velocity and direction of motion of a single dislocation are functions of the deformation applied to the three modes. Although here we focused our attention on the climb and glide mechanisms, more general situations

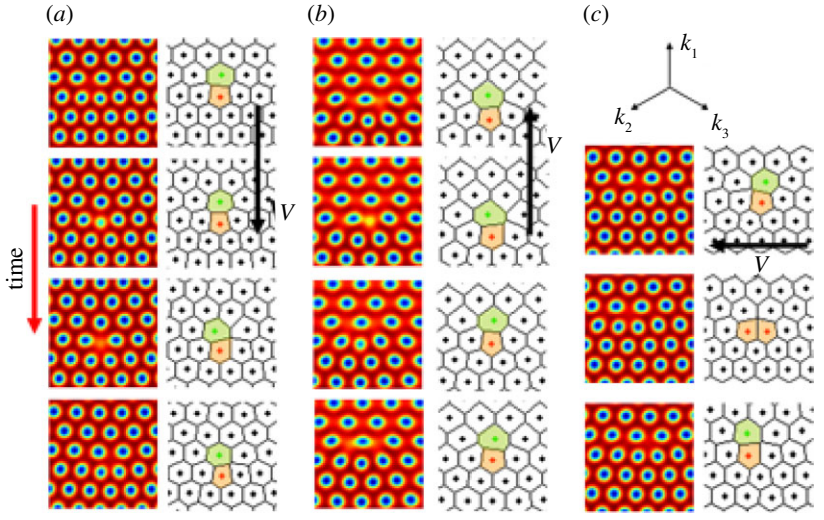

Figure 5. Mechanisms of defect motion in hexagonal patterns as seen through $\psi(\mathbf{r})$ (left) and their associated Voronoi diagrams (right) for three different perturbations ($\tau - \tau_c = 10^{-4}$). In the Voronoi diagrams, the orange cells are five-sided and the green cells are seven-sided. The defect moves through a series of T1 and T2 elementary processes, cell mitosis and near-neighbour switching. (*a*) $K_2 = K_3 > 0$. (*b*) $K_2 = K_3 < 0$. (*c*) $K_2 = -K_3$. The arrows indicate the direction of motion of the dislocation. In (*a*) and (*b*), the dislocation moves via the climb mechanism, while in (*c*) the dislocation glides horizontally. (Online version in colour.)

can easily be analysed. The process of defect motion under different deformations is illustrated through the order parameter ψ and the corresponding Voronoi diagrams in figure 5.

Theoretical and numerical results of Tsimring's theory [42] showed that, when the wavenumber corrections of the two striped patterns with dislocations are equal and non-zero ($\mathbf{K}_2$ and $\mathbf{K}_3$), the motion of the dislocation is parallel to the wavevector of the dislocation-free stripes $\mathbf{k}_1$.

Figure 5 shows the mechanism involved in the motion of dislocations for $K_1 = 0$, and $K_2 = K_3 > 0$. In good agreement with Tsimring's theory, we found that in this case the motion of the dislocation is parallel to $\mathbf{k}_1$. In the case that both $\mathbf{K}_2$ and $\mathbf{K}_3$ point in the same directions as $\mathbf{k}_2$ and $\mathbf{k}_3$, respectively, the dislocation moves in the direction that adjusts the wavenumber of the pattern back into the stability region by removing the extra stripes of $\mathbf{k}_2$ and $\mathbf{k}_3$, thereby moving the dislocation core antiparallel to $\mathbf{k}_1$. Then, the dislocation moves in the direction that reduces both $\mathbf{K}_2$ and $\mathbf{K}_3$ at the same rate.

For the case when $K_1 = K_2 < 0$, the dislocation moves in the direction that adjusts the wavenumber of the pattern by adding an extra stripe to the modes $\mathbf{k}_2$ and $\mathbf{k}_3$. In this case, the dislocation velocity is parallel to $\mathbf{k}_1$ and its motion results from the division of heptagonal cells by the so-called mitosis mechanism [43].

The motion of the dislocation involves the elimination of two rows of hexagonal domains by alternately eliminating a cell from rows perpendicular to the $\mathbf{k}_2$ and $\mathbf{k}_3$ directions. The result of the process is a zig-zag motion, the average direction of which is parallel to $\mathbf{k}_1$. In this case, the motion of the dislocation involves a series of T1 and T2 intermediate processes (e.g. Weaire & Rivier [44]). In addition, we

have observed that the direction of motion of the dislocation is not affected by small changes in the wavenumber K_1. Both results are in good agreement with the theoretical results of Tsimring [42].

We also analyse the case where $\mathbf{K}_2$ points in the same direction as $\mathbf{k}_2$, but $\mathbf{K}_3$ points in the opposite direction to $\mathbf{k}_3$. In this case, in order to push back the system into equilibrium, the motion of the dislocation is perpendicular to the wavevector of the dislocation-free wavevector $\mathbf{k}_1$ (glide mechanism).

The dynamics of dislocations in crystalline structures of different symmetries has been studied through different phase field models. For example, it was found that for the Swift–Hohenberg dynamics [45] the climb velocity is proportional to $K^{3/2}$, while in patterns with hexagonal, square or dodecagonal symmetry with a dynamics governed by the Lifshitz–Petrich model the climb velocity is proportional to the wavenumber disturbance ($v \sim K$) [46,47]. A similar result was found by Berry *et al.* [48] by means of a different phase field model for a conserved order parameter. In this study, the mechanisms of glide, climb and defect annihilation were analysed for hexagonal crystals subjected to different strain fields. By measuring the dislocation's glide and climb velocities as a function of the average shear strain γ, these authors found that $v \sim \gamma$.

On the other hand, the dynamics of dislocations in quasi-two-dimensional systems has been experimentally studied in Bénard–Marangoni convection systems [43] and in a single layer of equal-sized soap bubbles [49]. Experimentally, it has also been found in different metals that the glide velocity is generally well described by $v \sim \gamma^m$, where m is the glide exponent, typically $m \sim 1$–5 for pure metals, although different defects, such as vacancies or interstitials, can profoundly modify these values [50].

Figure 6 shows the velocity of the dislocations as a function of the wavenumber distortions for the three different deformations shown in figure 5. Irrespective of the deformation of the system, the velocity increases according to a power law with the wavenumber, with an exponent close to 2.5 ($v \sim K^{(2.5-2.8)}$).

In figure 6, we can also observe that the mechanism involving the glide of the dislocation is almost one order of magnitude faster than the process involving the climb of the dislocation. In addition, given that the mechanisms involved in the climb process for parallel or antiparallel motion are different, for a given deformation the resulting velocity is larger for a system where the motion is parallel to $\mathbf{k}_1$.

Irrespective of the mechanism of diffusion, here it was found that the motion of the dislocations at low velocities involves alternate stick–slip steps, while it becomes nearly continuous at relatively high deformations, in good agreement with the results reported by Berry *et al.* [48].

Finally, we have also analysed the dynamics of defect annihilation in the absence of any external distortion. When two dislocations interact, they may attract, repel or recombine in a new dislocation with a different Burgers vector. In the appropriate conditions, the collision of pairs of dislocations with opposite Burgers vectors may remove the dislocations, leaving the hexagonal pattern free of topological disturbances. In figure 7, the distance between the cores of two dislocations with opposite Burgers vectors is shown as a function of time. In very good agreement with Tsimring's theoretical and numerical results, here we found that the data are consistent with $R \propto (t_0 - t)^{1/2}$, where t_0 in the annihilation time of the pair of dislocations. Then, the velocity scales with the

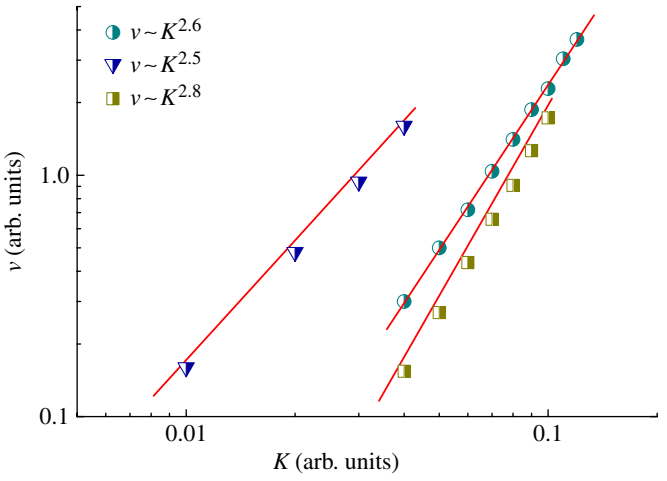

Figure 6. Dependence of the defect velocity on the wavenumber K for glide (triangles, $K_2 = -K_3$) and climb (squares, $K_2 = K_3 < 0$, and circles, $K_2 = K_3 > 0$). Irrespective of the mechanism of diffusion, the velocity of the dislocation grows according to a power law with K (solid lines). Here $\tau - \tau_c = 10^{-4}$. (Online version in colour.)

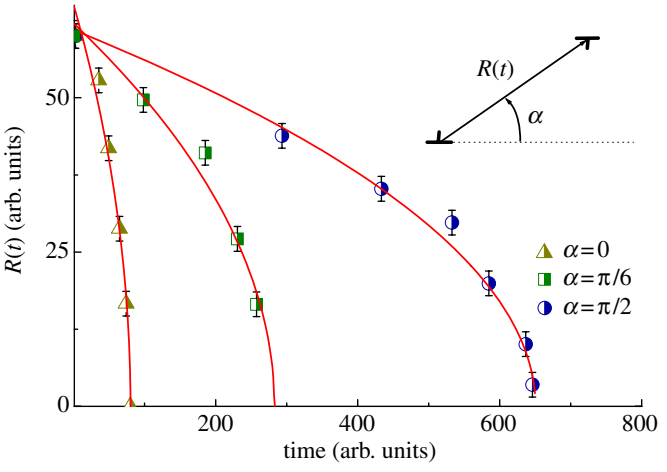

Figure 7. Temporal evolution of the average distance between dislocations during a process of annihilation ($\tau - \tau_c = 10^{-4}$, $K = 0$). Note that, at zero angle, the dislocations annihilate more quickly via the glide mechanism. (Online version in colour.)

distance between dislocations as $V \propto R^{-1}$. Assuming that the dynamics of defect diffusion is overdamped, the force F_{ds} between dislocations must decrease with the distance between defects as $F_{ds} \propto R^{-1}$, in good agreement with the theory of crystal elasticity [50]. Since the glide velocity is approximately one order of magnitude faster than the motion involving the climb mechanism, for the configuration studied here, there is a strong dependence of the annihilation time on the dominant direction of motion. A similar dependence on the direction of motion was found by Tsimring [51] in the framework of coupled amplitude equations for hexagonal patterns.

5. Summary

In thin films of block copolymers with hexagonal symmetry, the length-scale selectivity and degree of order are principally governed by the density and distribution of dislocations. Here, we have studied the dynamics of dislocation motion through a phase field model for a diblock copolymer. It was found that the fundamental mechanisms involved in the motion of dislocations are similar to those found in different phase field models and experimental systems. However, we found that the motion of dislocations is more strongly dependent on the external deformation, indicating that the dynamics is very sensitive to the details of the free-energy functional. The Ohta–Kawasaki model employed here is one of the simplest possible models to analyse the dynamics of phase separation and coarsening in block copolymer thin films. Recent experiments on sphere-forming and cylinder-forming block copolymer thin films have demonstrated that both systems respond to a shearing field, orienting the patterns in a direction dictated by the external shear [14,52]. It has been found that a minimum threshold stress is required to induce orientational order in the thin film and that the alignment quality is limited only by the residual isolated dislocations. It is hoped that this work will stimulate experimental research to study the motion of dislocations in block copolymer thin films under the conditions analysed. It is anticipated that more realistic models, including, for example, a more accurate description of the free-energy functional, asymmetry in the A and B statistical segment lengths, effective monomeric friction coefficients, and thermal fluctuations, could make the motion of dislocations yet more complex and dynamically rich.

This work was supported by Universidad Nacional del Sur (UNS), the National Research Council (CONICET) and the National Agency for Scientific and Technological Promotion (ANPCyT) of Argentina.

References

1 Helfand, E. 1975 Theory of inhomogeneous polymers: fundamentals of the Gaussian random-walk model. *J. Chem. Phys.* **62**, 999–1006. (doi:10.1063/1.430517)
2 Matsen, M. W. & Bates, F. S. 1996 Origins of complex self-assembly in block copolymers. *Macromolecules* **29**, 7641–7644. (doi:10.1021/ma960744q)
3 Matsen, M. W. & Bates, F. S. 1997 Block copolymer microstructures in the intermediate-segregation regime. *J. Chem. Phys.* **106**, 2436–2449. (doi:10.1063/1.473153)
4 Bates, F. S. & Fredrickson, G. H. 1999 Block copolymers—designer soft materials. *Phys. Today* **52**, 32–38. (doi:10.1063/1.882522)
5 Hamley, I. W. 1998 *The physics of block copolymers*. Oxford, UK: Oxford University Press.
6 Harrison, C., Adamson, D. H., Cheng, Z., Sebastian, J. M., Sethuraman, S., Huse, D. A., Register, R. A. & Chaikin, P. M. 2000 Mechanisms of ordering in striped patterns. *Science* **290**, 1558–1560. (doi:10.1126/science.290.5496.1558)
7 Harrison, C., Cheng, Z., Sethuraman, S., Huse, D. A., Chaikin, P. M., Vega, D. A., Sebastian, J. M., Register, R. A. & Adamson, D. H. 2002 Dynamics of pattern coarsening in a two-dimensional smectic system. *Phys. Rev. E* **66**, 011706. (doi:10.1103/PhysRevE.66.011706)
8 Harrison, C. 2004 Pattern coarsening in a 2D hexagonal system. *Europhys. Lett.* **67**, 800–808. (doi:10.1209/epl/i2004-10126-5)
9 Segalman, R. A., Hexemer, A., Hayward, R. C. & Kramer, E. J. 2003 Ordering and melting of block copolymer spherical domains in 2 and 3 dimensions. *Macromolecules* **36**, 3272–3288. (doi:10.1021/ma021367m)

10 Segalman, R. A., Hexemer, A. & Kramer, E. J. 2003 Edge effects on the order and freezing of a 2D array of block copolymer spheres. *Phys. Rev. Lett.* **91**, 196101. (doi:10.1103/PhysRevLett.91.196101)

11 Segalman, R. A. 2005 Patterning with block copolymer thin films. *Mater. Sci. Eng. Rep.* **48**, 191–196. (doi:10.1016/j.mser.2004.12.003)

12 Hamley, I. W. 2003 Nanostructure fabrication using block copolymers. *Nanotechnology* **14**, R39–R54. (doi:10.1088/0957-4484/14/10/201)

13 Angelescu, D. E., Waller, J. H., Register, R. A. & Chaikin, P. M. 2005 Shear-induced alignment in thin films of spherical nanodomains. *Adv. Mater.* **17**, 1878–1881. (doi:10.1002/adma.200401994)

14 Marencic, A. P., Wu, M. W., Register, R. A. & Chaikin, P. M. 2007 Orientational order in sphere-forming block copolymer thin films aligned under shear. *Macromolecules* **40**, 7299–7305. (doi:10.1021/ma0713310)

15 Kramer, E. J. 2005 Condensed-matter physics: melted by mistakes. *Nature* **437**, 824–825. (doi:10.1038/437824b)

16 Vega, D. A., Harrison, C. K., Angelescu, D. E., Trawick, M. L., Huse, D. A., Chaikin, M. P. & Register, R. A. 2005 Ordering mechanisms in two-dimensional sphere-forming block copolymers. *Phys. Rev. E* **71**, 061803. (doi:10.1103/PhysRevE.71.061803)

17 Gómez, L. R., Vallés, E. M. & Vega, D. A. 2006 Lifshitz–Safran coarsening dynamics in a 2D hexagonal system. *Phys. Rev. Lett.* **97**, 188302. (doi:10.1103/PhysRevLett.97.188302)

18 Pezzutti, A. D., Gomez, L. R., Villar, M. A. & Vega, D. A. 2009 Defect formation during a continuous phase transition. *Europhys. Lett.* **87**, 66003. (doi:10.1209/0295-5075/87/66003)

19 Lifshitz, L. M. 1962 Kinetics of ordering during second-order phase transitions. *Sov. Phys. J. Exp. Theor. Phys.* **15**, 939–942.

20 Safran, S. A. 1981 Domain growth of degenerate phases. *Phys. Rev. Lett.* **46**, 1581–1585. (doi:10.1103/PhysRevLett.46.1581)

21 Gómez, L. R., Vallés, E. M. & Vega, D. A. 2007 Effect of thermal fluctuations on the coarsening dynamics of 2D hexagonal system. *Physica A* **386**, 648–654. (doi:10.1016/j.physa.2007.08.056)

22 Ferrero, E. E. & Cannas, S. A. 2007 Long-term ordering kinetics of the two-dimensional q-state Potts model. *Phys. Rev. E* **76**, 031108. (doi:10.1103/PhysRevE.76.031108)

23 Gómez, L. R. 2009 PhD thesis. Universidad Nacional del Sur, Bahía Blanca, Argentina.

24 Cahn, J. & Hilliard, J. E. 1958 Free energy of a nonuniform system. *J. Chem. Phys.* **28**, 258–266. (doi:1063/1.1744102)

25 Ohta, T. & Kawasaki, K. 1986 Equilibrium morphology of block copolymer melts. *Macromolecules* **19**, 2621–2632. (doi:10.1021/ma00164a028)

26 Ohta, T. & Kawasaki, K. 1990 Comment on the free energy functional of block copolymer melts in the strong segregation limit. *Macromolecules* **23**, 2413–2414. (doi:10.1021/ma00210a047)

27 Ren, S. R. & Hamley, I. W. 2001 Cell dynamics simulations of microphase separation in block copolymers. *Macromolecules* **34**, 116–126. (doi:10.1021/ma000678z)

28 Kodama, H. & Doi, M. 1996 Shear-induced instability of the lamellar phase of a block copolymer. *Macromolecules* **29**, 2652–2658. (doi:10.1021/ma9512216)

29 Bray, A. J., Cavagna, A. & Travasso, R. D. M. 2001 Interface fluctuations, Burgers equations, and coarsening under shear. *Phys. Rev. E* **65**, 016104. (doi:10.1103/PhysRevE.65.016104)

30 Leibler, L. 1980 Theory of microphase separation in block copolymers. *Macromolecules* **13**, 1602–1617. (doi:10.1021/ma60078a047)

31 Brazovskii, S. A. 1975 Phase transition of an isotropic system to a nonuniform state. *Sov. Phys. J. Exp. Theor. Phys.* **41**, 85–89.

32 Fredrickson, G. H. & Helfand, E. 1987 Fluctuation effects in the theory of microphase separation in block copolymers. *J. Chem. Phys.* **87**, 697–705. (doi:10.1063/1.453566)

33 Podneks, V. E. & Hamley, I. W. 1996 Landau–Brazovskii model for the Ia$\bar{3}$d structure. *J. Exp. Theor. Phys. Lett.* **64**, 618–624. (doi:10.1209/0295-5075/87/66003)

34 Oono, Y. & Shiwa, Y. 1987 Computationally efficient modeling of block copolymer and Bénard pattern formations. *Mod. Phys. Lett. B* **1**, 49–55. (doi:10.1142/S0217984987000077)

35 Oono, Y. & Puri, S. 1988 Study of phase-separation dynamics by use of cell dynamical systems. I. Modeling. *Phys. Rev. A* **38**, 434–453. (doi:10.1103/PhysRevA.38.434)
36 Puri, S. & Oono, Y. 1988 Study of phase-separation dynamics by use of cell dynamical systems. II. Two-dimensional demonstrations. *Phys. Rev. A* **38**, 1542–1575. (doi:10.1103/PhysRevA.38.1542)
37 Bahiana, M. & Oono, Y. 1990 Cell dynamical system approach to block copolymers. *Phys. Rev. A* **41**, 6763–6771. (doi:10.1103/PhysRevA.41.6763)
38 Vega, D. A. & Gomez, L. R. 2009 Relaxational dynamics of smectic phases on a curved substrate. *Phys. Rev. E* **79**, 031701. (doi:10.1103/PhysRevE.79.031701)
39 Qi, S. & Wang, Z. 1996 Kinetic pathways of order–disorder and order–order transitions in weakly segregated microstructured systems. *Phys. Rev. Lett.* **76**, 1679–1683. (doi:10.1103/PhysRevLett.76.1679)
40 Sushchik, M. M. & Tsimring, L. S. 1994 The Eckhaus instability in hexagonal patterns. *Physica D* **74**, 90–106. (doi:10.1016/0167-2789(94)90028-0)
41 Boyer, D. & Vigals, J. 2002 Weakly nonlinear theory of grain boundary motion in patterns with crystalline symmetry. *Phys. Rev. Lett.* **89**, 055501. (doi:10.1103/PhysRevLett.89.055501)
42 Tsimring, L. S. 1996 Dynamics of penta–hepta defects in hexagonal patterns. *Physica D* **89**, 368–380. (doi:10.1016/0167-2789(95)00222-7)
43 Semwogerere, D. & Schatz, M. F. 2002 Evolution of hexagonal patterns from controlled initial conditions in a Bénard–Marangoni convection experiment. *Phys. Rev. Lett.* **88**, 054501. (doi:10.1103/PhysRevLett.88.054501)
44 Weaire, D. & Rivier, N. 1984 Soap, cells and statistics—random patterns in two dimensions. *Contemp. Phys.* **25**, 59–99. (doi:10.1080/00107518408210979)
45 Swift, J. B. & Hohenberg, P. C. 1977 Hydrodynamic fluctuations at the convective instability. *Phys. Rev. A* **15**, 319–328. (doi:10.1103/PhysRevA.15.319)
46 Cross, M. C. & Hohenberg, P. C. 1993 Pattern formation outside of equilibrium. *Rev. Mod. Phys.* **65**, 851–1112. (doi:10.1103/RevModPhys.65.851)
47 Barak, G. & Lifshitz, R. 2006 Dislocation dynamics in a dodecagonal quasiperiodic structure. *Phil. Mag.* **86**, 1059–1064. (doi:10.1080/14786430500256383)
48 Berry, J. M., Grant, M. & Elder, K. R. 2006 Diffusive atomistic dynamics of edge dislocations in two dimensions. *Phys. Rev. E* **73**, 031609. (doi:10.1103/PhysRevE.73.031609)
49 Tam, T., Ohata, D. & Wu, M. 2000 Dynamics of a penta–hepta defect in a hexagonal pattern. *Phys. Rev. E* **61**, R9–R12. (doi:10.1103/PhysRevE.61.R9)
50 Amodeo, R. J. 1990 Dislocation dynamics. A proposed methodology for deformation micromechanics. *Phys. Rev. B* **41**, 6958–6967. (doi:10.1103/PhysRevB.41.6958)
51 Tsimring, L. S. 1995 Penta–hepta defect motion in hexagonal patterns. *Phys. Rev. Lett.* **74**, 4201–4204. (doi:10.1103/PhysRevLett.74.4201)
52 Marencic, A. P., Adamson, D. H., Chaikin, P. M. & Register, R. A. 2010 Shear alignment and realignment of sphere-forming and cylinder-forming block-copolymer thin films. *Phys. Rev. E* **81**, 011503. (doi:10.1103/PhysRevE.81.011503)